Available online at www.sciencedirect.com

SCIENCE DIRECT®

Marine Chemistry 93 (2005) 131–147

MARINE CHEMISTRY

www.elsevier.com/locate/marchem

The continental shelf pump for CO_2 in the North Sea—evidence from summer observation

Yann Bozec*, Helmuth Thomas[1], Khalid Elkalay, Hein J.W. de Baar

Royal Netherlands Institute for Sea Research, Department of Marine Chemistry and Geology, P.O. Box 59, 0NL-1790 AB Den Burg, The Netherlands

Received 2 February 2004; received in revised form 29 June 2004; accepted 9 July 2004
Available online 14 October 2004

Abstract

Data on the distribution of dissolved inorganic carbon (DIC) and partial pressure of CO_2 (pCO_2) were obtained during a cruise in the North Sea during late summer 2001. A 1° by 1° grid of 97 stations was sampled for DIC while the pCO_2 was measured continuously between the stations. The surface distributions of these two parameters show a clear boundary located around 54°N. South of this boundary the DIC and pCO_2 range from 2070 to 2130 μmol kg^{-1} and 290 to 490 ppm, respectively, whereas in the northern North Sea, values range between 1970 and 2070 μmol kg^{-1} and 190 to 350 ppm, respectively. The vertical profiles measured in the two different areas show that the mixing regime of the water column is the major factor determining the surface distributions. The entirely mixed water column of the southern North Sea is heterotrophic, whereas the surface layer of the stratified water column in the northern North Sea is autotrophic. The application of different formulations for the calculation of the CO_2 air–sea fluxes shows that the southern North Sea acts as a source of CO_2 for the atmosphere within a range of +0.8 to +1.7 mmol m^{-2} day^{-1}, whereas the northern North Sea absorbs CO_2 within a range of −2.4 to −3.8 mmol m^{-2} day^{-1} in late summer. The North Sea as a whole acts as a sink of atmospheric CO_2 of −1.5 to −2.2 mmol m^{-2} day^{-1} during late summer. Compared to the Baltic and the East China Seas at the same period of the year, the North Sea acts a weak sink of atmospheric CO_2. The anticlockwise circulation and the short residence time of the water in the North Sea lead to a rapid transport of the atmospheric CO_2 to the deeper layer of the North Atlantic Ocean. Thus, in late summer, the North Sea exports 2.2×10^{12} g C $month^{-1}$ to the North Atlantic Ocean via the Norwegian trench, and, at the same period, absorbs from the atmosphere a quantity of CO_2 ($0.4\ 10^{12}$ g C $month^{-1}$) equal to 15% of that export, which makes the North Sea a continental shelf pump of CO_2.

Keywords: North Sea; Dissolved inorganic carbon; CO_2 air–sea exchange; Continental shelf pump; Marginal seas

1. Introduction

Human activities have released vast amounts of the greenhouse gas carbon dioxide (CO_2) into the

* Corresponding author. Tel.: +31 222 369 439.
E-mail address: bozec@nioz.nl (Y. Bozec).
[1] Present address: Department of Oceanography, Dalhousie University, 1355 Oxford Street, Halifax, Nova Scotia, Canada, B3H 4J1.

0304-4203/$ - see front matter © 2004 Elsevier B.V. All rights reserved.
doi:10.1016/j.marchem.2004.07.006

atmosphere by fossil fuel burning and deforestation, which corresponds to ~5.4±0.3 petagrams of carbon per year (Pg C year^{-1}) (1 Pg=10^{15} g) during the 1980s. It is well established that 3.3±0.1 Pg C year^{-1} remain in the atmosphere (IPCC, 2001). The world ocean behaves as a sink estimated as 1.9±0.6 Pg C year^{-1}, and the terrestrial biosphere is assumed to trap the remaining 0.2±0.7 Pg C year^{-1} (IPCC, 2001). Since the land sink is usually considered as the closing term for the global budgeting, it is essential to reduce the uncertainties regarding the oceanic uptake of anthropogenic CO_2. The estimates of this uptake still vary significantly (Lee et al., 1998; Gruber and Keeling, 2001; Orr et al., 2001; Thomas et al., 2001). One of the reasons for this uncertainty could be that all these assessments ignore the CO_2 fluxes in the coastal oceans. Because of the small-scale variability observed in these regions, it has been difficult to consider coastal seas in global circulation models. Moreover, hitherto there has been a lack of field data on the spatial and temporal variability of dissolved inorganic carbon (DIC) and the partial pressure of CO_2 (pCO_2) for the coastal ocean.

The coastal ocean is known to house a disproportionately large fraction of the oceanic primary production of 15% to 30% (Walsh, 1991; Wollast, 1998), a contribution that is much larger than the contribution of coastal seas (7%) to the total ocean surface area. Thus, these regions strongly affect the global carbon cycle, however it has not been established yet whether they act as a sink or as a source of atmospheric CO_2 (Walsh, 1991; Smith and Hollibaugh, 1993; Kempe, 1995; Gattuso et al., 1998; Mackenzie et al., 1998; Wollast, 1998).

The North Sea has been the subject of intense investigations for many decades by several institutions, making this area one of the best understood coastal seas of the world. Very recent results by Thomas et al. (2004) showed that the North Sea acts as a sink for atmospheric CO_2 and export ≈93% of the absorbed CO_2 to the North Atlantic Ocean, therefore acting like a continental Shelf pump as described by Tsunogai et al. (1999) for the East China Sea. Thomas et al. (2004) suggested that during the late summer situation, the differences between the two biogeochemical regions with regard to the air-sea exchange of CO_2 are most prominent. A detailed investigation of the CO_2 system in this period is provided here in order to gain insight in the control mechanisms of the CO_2 air-sea exchange on the North Sea.

In the North Sea, previous investigations focused mainly on certain aspects related to the carbon cycle, e.g. primary production and the transport of organic matter within the North Sea (Postma and Rommets, 1984; Kempe et al., 1988). Pioneering investigations of the inorganic carbon cycle during summer 1986 had been done with potentiometric determination of DIC and alkalinity (Pegler and Kempe, 1988; Kempe and Pegler, 1991), upon which the alkalinity was used together with pH to calculate the pCO_2. Moreover, many other regional studies were conducted (Hoppema, 1990, 1991; Kempe and Pegler, 1991; Bakker et al., 1996; Frankignoulle et al., 1996a; Frankignoulle et al., 1996b; Frankignoulle et al., 1996c; Frankignoulle et al., 1998; Borges and Frankignoulle, 1999; Brasse et al., 1999; Borges and Frankignoulle, 2002; Brasse et al., 2002). However, the currently available carbon data sets for the entire North Sea still are sparse and do not allow unequivocal conclusions about the carbon cycle.

The bottom topography of the North Sea is likely to constitute the major control for biogeochemical cycling, in particular for inorganic carbon parameters: The deeper northern part reveals depths of approximately 150 m on the shelf, of 400 m in the Norwegian Channel and of 700 m in the Skagerrak (Fig. 1). In the southern part (south of 54°N), depths are less than 50 m and even less than 20 m near the coasts (Eisma, 1987). Because of the shallow conditions in the south, the water column is mixed throughout the year, while thermal stratification occurs in the northern part during summer. The spatial distribution of the carbonate system is also affected by the inorganic and organic carbon inputs from the estuaries. The southern part receives most of the freshwater inputs, notably from the rivers Rhine, Scheldt, Thames and Elbe (Fig. 1). Haline stratification is an exception in the northern part and only occurs in the Norwegian Trench area and in the vicinity of river inlets with strong freshwater input.

The main aim of the present study is to verify the hypothesis of a "continental shelf pump" for the uptake of atmospheric CO_2 with subsequent transport to the open ocean. Here we present a new compre-

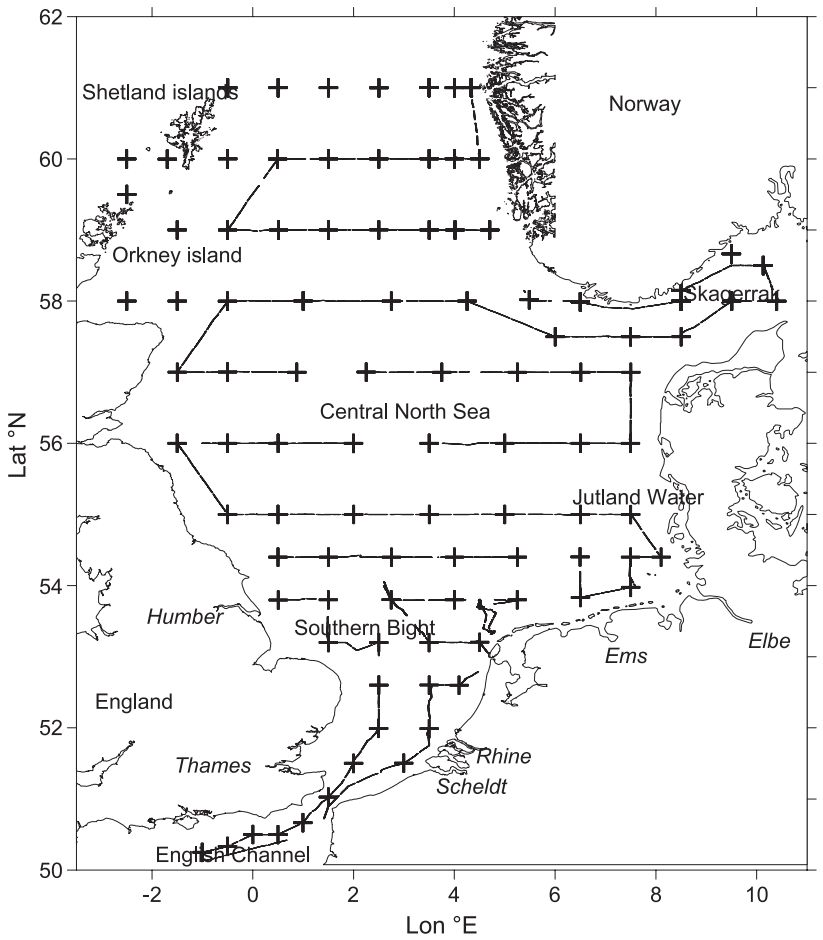

Fig. 1. Map of the study area. The North Sea was covered by an adapted 1° by 1° sampling grid of 97 stations (+). Between the stations, continuous measurements of temperature, salinity and pCO_2 were carried out (dotted line).

hensive study in the late summer of 2001, with improved accuracy relying on now available certified DIC standards, and direct measurements of pCO_2 which is calibrated versus certified gas mixtures. We also investigate the interactions between carbon, oxygen and nutrients in order to describe the "biological CO_2 pump". We can rely on a complete new data set with high spatial resolution for the carbonate system and related chemical, biological and physical parameters obtained during our cruise in the North Sea during late summer 2001.

In the present paper, we firstly describe the surface water distribution of the inorganic carbon system and for related parameters in the North Sea. In Section 4.1, we describe the different water masses, which govern these distributions. In Sections 4.2 and 4.3, we will focus on the differences in carbonate chemistry between the northern and the southern North Sea, respectively. In Section 4.4, we evaluate the monthly atmospheric CO_2 fluxes in both regions and assess, whether the North Sea acts as a source or a sink for CO_2 during late summer. Finally, in Section 4.5 we propose a mechanism of the continental shelf pump in the North Sea.

2. Material and methods

The data were obtained during a cruise in the North Sea (18.08.2001–13.09.2001), on board *RV Pelagia*.

The North Sea was covered by an adapted 1° by 1° grid with 97 stations (Fig. 1). This grid was specifically designed to focus on the relevant regions for biogeochemical cycles such as the Shetland and English Channels (inflow of North Atlantic water), the Skagerrak area (inflow of Baltic Sea water) and the western Scandinavian coast (outflow to the North Atlantic). The stations were also denser in the Southern Bight (Fig. 1) that receives the major freshwater inputs, whereas the station's distribution was sparser in the more homogenous central North Sea.

During this cruise, a total of 745 water samples were collected at the stations and the concentrations of DIC, oxygen and nutrient as well as chlorophyll *a* (from the surface water samples), salinity and temperature were determined. In the surface waters, salinity and temperature were determined continuously from the ship's water supply as well as the pCO_2 leading to a total of 22 000 surface measurements for this parameter (Fig. 1).

DIC samples from CTD casts were collected in 250 mL glass bottles, which were kept cold in the dark before measurement. The DIC concentrations were determined by the coulometric method of Johnson et al. (1993), as previously described by Stoll (1994). A new coulometric cell was prepared approximately every 12 h and calibrated versus Certified Reference Material (CRM) (batch #52). The accuracy and the precision of the system were controlled by the repeated measurement of CRM material before and after each station. Three to four replicates were determined of each sample and of each standard with a precision better than 1 μmol kg^{-1}.

The pCO_2 in the surface waters was determined using an underway system with continuous flow equilibration. The water flow from the pump was about 60 L min^{-1}, which was reduced by a bypass just before the equilibrator to 2–3 L min^{-1}. The temperature difference between the equilibrator and the surface water was less than 0.5 K, and usually 0.1 K. The detection of pCO_2 was performed by a non-dispersive infrared spectrometer, which was calibrated against *National Oceanic and Atmospheric Administration* (NOAA) standards every 24 h. The method is described in detail by Körtzinger et al. (1996) with an estimated error of approximately 1 μatm. The atmospheric pCO_2 was sampled at the antenna platform of the ship and determined every 2 h.

Nitrate (NO_3^-), nitrite (NO_2^-) and phosphate (PO_4^{3-}) were analysed in all samples within 10 h after sampling, using a technicon TRAACS 800 autoanalyser according to Grasshoff et al. (1983). The standard deviation for the sum of NO_3^- and NO_2^- ($NO_{2/3}$) was ±0.02 μM and for PO_4^{3-} ±0.01 μM. The estimated accuracy were ±1.5% and 3%, respectively.

The oxygen concentration was measured by the Winkler method using a potentiometric end-point determination with an estimated accuracy of ±2 μmol kg^{-1} (±0.5% of level of saturation). The oxygen saturation level ($\%O_2$) and the apparent oxygen utilization (AOU) were calculated from the observed concentrations of dissolved O_2 and the concentrations of O_2 at saturation using the algorithm proposed by Weiss (1970).

The sea-surface temperature and salinity were measured continuously with an AQUAFLOW thermo-salinograph with the water intake at a depth of about 3 m. Temperature and salinity were calibrated vs. the CTD measurements.

The concentration of chlorophyll *a* was determined from GF/F filtered samples by the fluorimetric method based on the method by Holm-Hansen et al. (1965) with a precision of ±4%.

3. Observations

3.1. Temperature and salinity

The continuous measurements of salinity and temperature during the cruise allowed us to plot high-resolution maps of these parameters in the surface water of the North Sea. A clear gradient of decreasing temperature is present in the North Sea from the southeast to the northwest (Fig. 2A). Highest temperatures between 18 and 19.2 °C were observed in the shallow southern and southeastern area, i.e., in the coastal areas, which receive large freshwater inputs from the English, Belgian, Dutch, German, and Danish coasts. High temperatures were also observed in the Skagerrak area, where high inputs of less saline water from the Baltic Sea and from the Norwegian coast occur. Lower temperatures were observed off the Humber estuary. The northern and northwestern parts were characterized by temperatures of 11 to 15 °C. These low values, especially in the

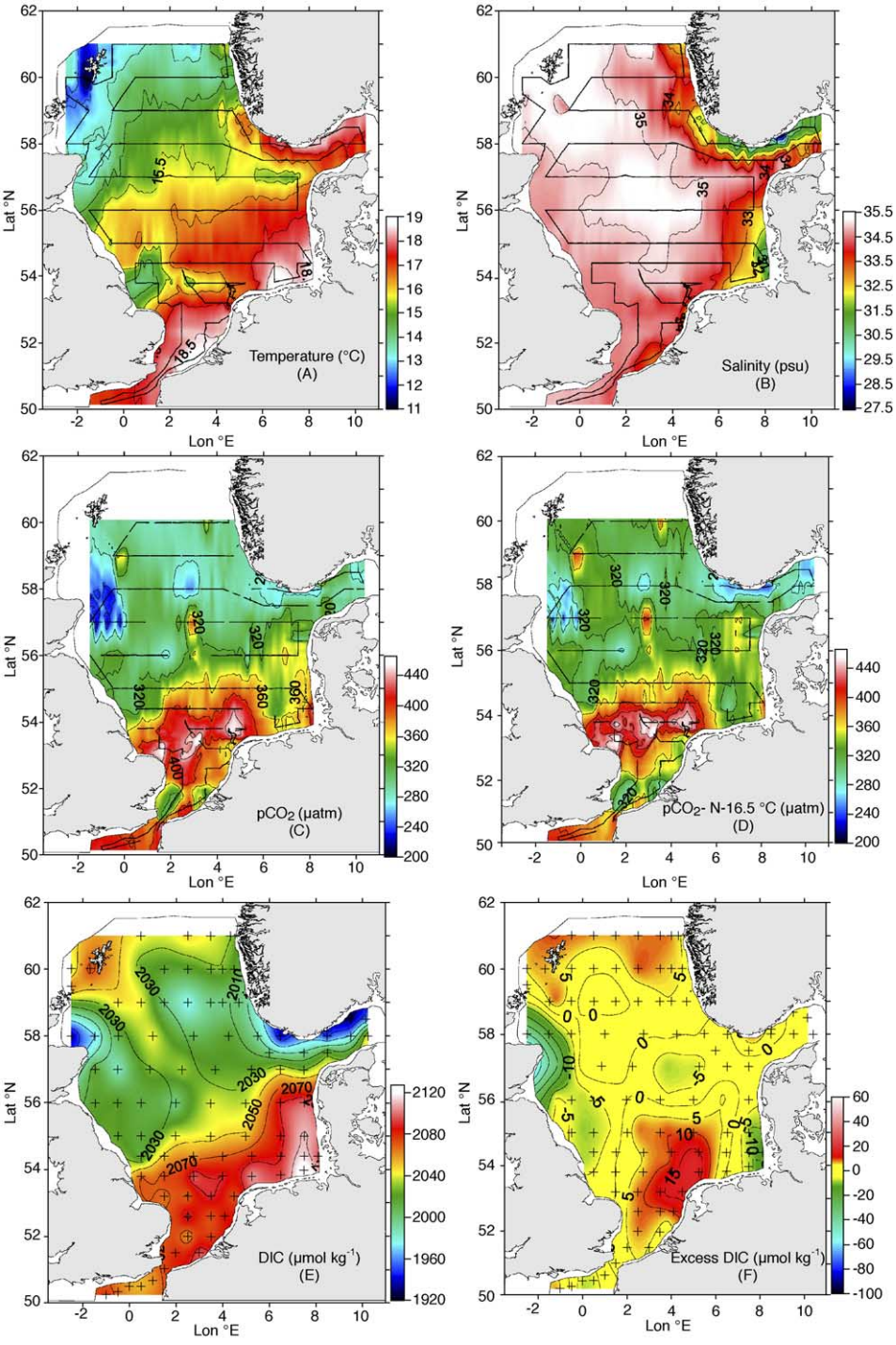

Fig. 2. Surface maps of temperature (A), salinity (B), the partial pressure of CO_2 (C), the partial pressure of CO_2 normalised to 16.5 °C (D), DIC (E) and excess DIC (F). For (A), (B), (C) and (D), the black line represents the continuous measurements for these parameters. The crosses on (E) and (F) represent the sampled stations for DIC.

Shetlands Islands Channel, indicate water input from the North Atlantic Ocean via the northern boundary of the North Sea.

West of the 4°E meridian, the North Sea is rather homogeneous in its surface salinity distribution with an average value of 34.5 (Fig. 2B), except off the Scheldt estuary, where riverine water inputs resulted in a salinity of 32.8. Highest salinities (35.1) were observed close to the North Sea's boundaries with the Atlantic Ocean in the north and in the English Channel. East of the 4°E meridian, the North Sea is characterized by lower salinity: Waters in the German Bight and in the adjacent Jutland waters had an average salinity of 32. Waters with lowest salinity of 27 were found in the Skagerrak area along the Norwegian south coast due to large inputs of less saline Baltic Sea water.

3.2. Observations of the CO_2 system and nutrients

The pCO_2 data recorded during the cruise allow us to plot the first high-resolution map of pCO_2 for the North Sea in late summer (Fig. 2C). Two different features of the pCO_2 distribution in the surface waters were observed, separating the North Sea in a southern and a northern region. In the south, pCO_2 was super-saturated relative to the atmosphere (atmospheric CO_2 value of 365 µatm) with values between 400 and 450 µatm. Highest values of pCO_2 were found in the German Bight and in the English Channel. The system changes from super-saturation to under-saturation in northward direction at approximately 54°N, where the North Sea becomes deeper and stratified. Thus, in the north the dominant feature was a strong CO_2 under-saturation of the surface waters with lowest values for the pCO_2 of 220 µatm observed in the Skagerrak area and the most northern region. The major features of the pCO_2 distribution remain visible after normalization of the pCO_2 values to the average temperature of 16.5 °C (Fig. 2D).

The DIC data show a similar pattern in surface waters (Fig. 2E). Higher concentrations relative to the Central North Sea were found in the southern part with values of 2070 µmol kg^{-1} in the English Channel, 2100 µmol kg^{-1} along the Belgian, Dutch and southern English coasts, with a maximum of 2130 µmol kg^{-1} in the German Bight. High concentrations relative to the rest of the North Sea were found locally off the main estuaries: DIC concentrations were 2099, 2081, 2096, 2108 and 2130 µmol kg^{-1} for the stations off the Scheldt, Thames, Humber, Ems and Elbe estuaries, respectively. Lower concentrations were found in the northern region of the North Sea, where the DIC concentration ranged from 1930 to 2070 µmol kg^{-1}. Lowest values were found in the Skagerrak and near the Scottish coast, whereas higher concentrations relative to the rest of the northern North Sea were found at the North Atlantic Water inputs in the Shetland Channel and in the northwestern region.

The excess DIC (Fig. 2F) has been calculated using the two linear regressions in Fig. 3. We used the equation established for the Skagerrak area to calculate the DIC expected from a conservative mixing in the northern North Sea (54°N–61°N) and the equation established in the Southern Bight to calculate the DIC expected from a conservative mixing in the southern North Sea (51°N–54°N). The difference between the DIC measured and the DIC calculated gives the excess DIC. The surface map of excess DIC (Fig. 2F) shows similar trend than the DIC surface map (Fig. 2E) with positive values in the southern North Sea and mainly negative values in the northern North Sea. The excess DIC allows us to identify the processes responsible for the DIC concentration observed in areas with important mixing such as the Southern Bight or Skagerrak area and will be discussed more in details in Sections 4.2 and 4.3.

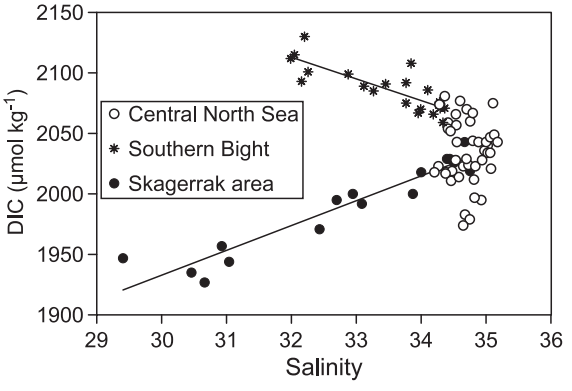

Fig. 3. Plots of surface water DIC versus salinity from CTD casts in the Central North Sea (○), Skagerrak area (●) and Southern Bight (*). Linear regression fits have the equations: DIC=−17.9S+2685 (n=20, r^2=0.7) for the Southern Bight and DIC=20.5S+1318 (n=17, r^2=0.9) for the Skagerrak.

Table 1
Characteristics of the three main water masses influencing the surface water distribution of carbon dioxide during late summer

	Southern Bight	Central North Sea	Skagerrak
Salinity	31.2–34.5	≈35	27.2–34.5
Temperature (°C)	14.0–19.2	11.0–16.0	16.5–19.0
DIC (μmol kg^{-1})	2060–2130	2000–2070	1930–2030
pCO_2 (μatm)	290–490	220–350	190–300
$NO_{3/2}$ (μM)	0–4.70	0–0.20	0–0.20
PO_4^{3-} (μM)	0–1.00	0–0.05	0–0.04

For each parameter, its concentration range in the surface layer is given for the 97 stations.

In late summer, at the end of the productive period the inorganic nutrients nitrate and phosphate were exhausted almost in the entire North Sea. South of 54°N the concentrations increased to 0.6 μM for NO_{32} and 0.3 μM for PO_4^{3-}. In certain areas close to the estuaries of the rivers Thames, Scheldt, Humber and Elbe their concentrations were somewhat elevated up to 5 μM for $NO_{3/2}$ and 1 μM for PO_4^{3-}. Moreover, the areas directly affected by inputs of North Atlantic Ocean waters (English and Shetland islands Channels) show higher $NO_{3/2}$ concentration up to 3 μM (Table 1).

4. Results and discussion

4.1. Dissolved inorganic carbon versus salinity

The relationship between DIC and salinity is exploited in order to investigate the DIC water mass characteristics in the North Sea (Fig. 3). In the surface waters, the DIC/salinity relationship indicates the three main water masses in the North Sea, which govern the inorganic carbon distribution during late summer:

(1) The Central North Sea water, which has similar characteristics to the North Atlantic water of high salinity (≈35) and DIC concentrations between 2050 and 2070 μmol kg^{-1}.
(2) The Southern Bight water mass, which is influenced by the riverine water input from the southern English, Belgian, Dutch, German and Danish coasts. Accordingly, it has lower salinities (30–34) and high DIC concentrations compared to the central North Sea, between 2090 and 2130 μmol kg^{-1}.
(3) The Skagerrak water mass, which is formed by the outflowing water from the Baltic Sea and riverine water input from the southern Norwegian coast. It has lower salinities (30–34) and DIC concentrations between 1930 and 2030 μmol kg^{-1}.

Two linear trends can be obtained from the DIC–salinity scatter plot (Fig. 3): one, with a negative slope encompassing the data from the Southern Bight and one with a positive slope which includes the samples from the Skagerrak and the southern Norwegian coast. Both regressions converge towards the Central North Sea water mass and represent the mixing of these three water masses.

The corresponding source water masses with DIC concentrations between 2090 and 2130 μmol kg^{-1} originate from the NW European, "lime-rich" continental landmass. The Baltic Sea water is characterized by low DIC concentrations relative to the two other water masses. In the Baltic Proper, the low DIC surface water from the Scandinavian coast (originating from lime poor drainage areas) mixes with relatively high DIC surface water from the southeastern Baltic Proper (originating from lime-rich drainage areas) as reported by Thomas and Schneider (1999) and Thomas et al. (2003a). Characteristics of these three water masses are given in Table 1.

4.2. The CO_2 system in the northern North Sea

In order to explain the differences in pCO_2 and DIC concentrations between the northern and the southern North Sea, it is important to consider the influence of the bottom topography of the North Sea, which constitutes a major control for the biogeochemical cycling.

Profiles of DIC in the northern part of the North Sea showed a clear stratification of the water column, with low concentrations in the surface layer and higher concentrations in the deeper layer (Fig. 4A, see also Fig. 6B). The low DIC values in the surface layer were related to negative apparent oxygen utilization (AOU), i.e., oxygen production (Figs. 4B and 5), and depleted $NO_{3/2}$ and PO_4^{3-} conditions (Fig. 4C and D). This indicates DIC, i.e., CO_2, NO_3^- and PO_4^{3-} consumption as well as

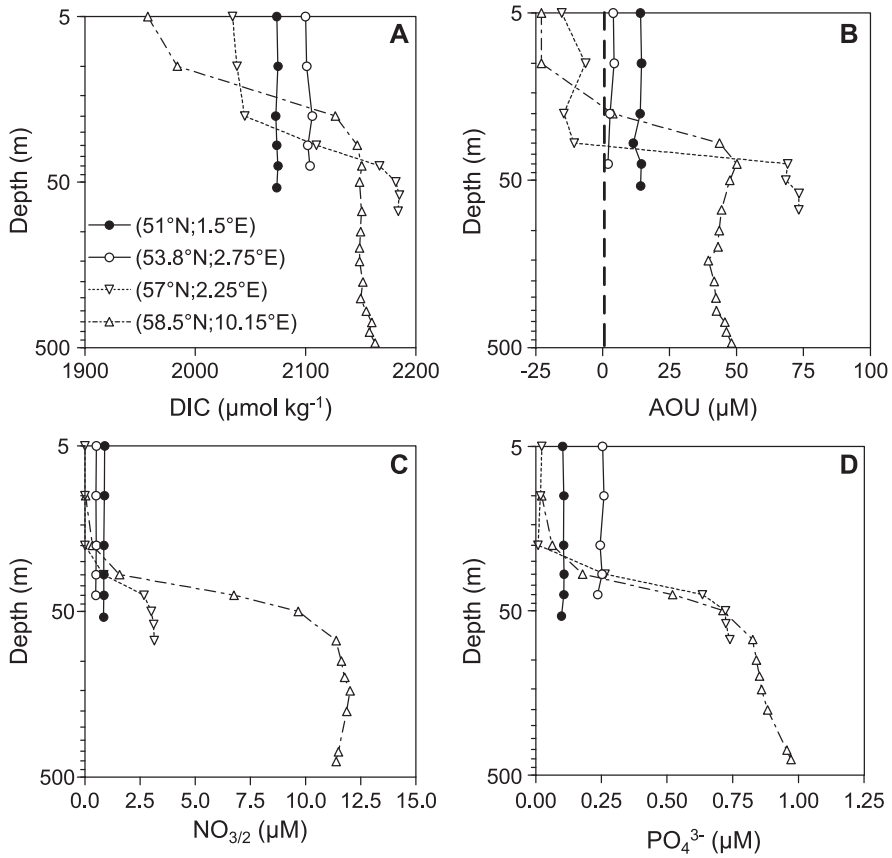

Fig. 4. Profiles of DIC (A), AOU (B), $NO_{3/2}$ (C) and PO_4^{3-} (D) in the southern and northern North Sea. Stations were situated at 51.00°N; 1.50°E (●), 53.80°N; 2.75°E (○), 57.00°N; 2.25°E (▽) and 58.50°N; 10.15°E (△). Depths are shown on a logarithmic scale.

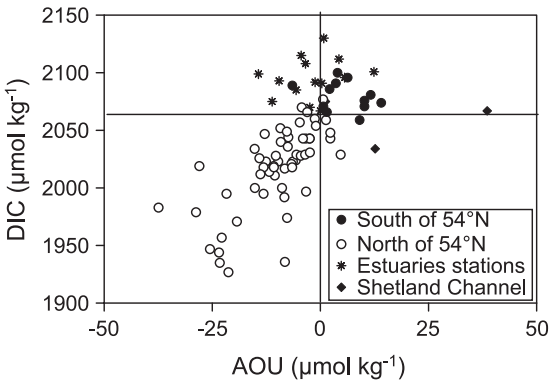

Fig. 5. DIC plotted versus AOU at 5 m depth in the North Sea, south of 54°N (●), north of 54°N (○), influenced by freshwater inputs (*) and in the Shetland Channel (◆).

oxygen release by primary production. In the northern North Sea, the biological production dominates the remineralization in the autotrophic upper layer of the water column and controls the CO_2 distribution. On the other hand, the increase in DIC concentrations within the deeper layer was caused by remineralization of organic matter, which had been exported to the deeper layer, as seen from the positive AOU and the increasing $NO_{3/2}$ and PO_4^{3-} concentrations in the deeper layer (see also Thomas et al., 1999; Osterroht and Thomas, 2000). This strong remineralization of particulate organic matter (POM) is predominant in the deeper layer of the northern North Sea, which makes this part of the water column heterotrophic. A direct consequence is that only a minor amount of carbon accumulates in the bottom sediments, which accounts for only less than 1% of the primary

production in the North Sea (De Haas, 1997; De Haas et al., 2002).

In the Skagerrak area, at the transition to the Baltic Sea, the excess DIC value of approximately zero (Fig. 2F) implies that the DIC concentrations found for the area are in the expected range when the less saline water from the Baltic sea mixes with Central North Sea water. The average value of 1900 μmol kg^{-1} found for DIC in this area is also in good agreement with values reported by Thomas and Schneider (1999). For the same range of salinity, between 30 and 31, these authors reported a similar value of 1900 μmol kg^{-1} in summer. This value is the result of biological production occurring in both the surface waters of the Baltic and the North Seas during spring and early summer, then mixed in the Skagerrak area.

Fig. 2C and E show that along the northern Scottish coast and near the Shetland Islands, the DIC and pCO_2 are different from those in the more homogeneous central North Sea:

At the stations located at 58°N; 2.5°W and 58°N; 1.5°W, surface water DIC concentrations were around 1950 μmol kg^{-1} and pCO_2 was as low as 220 μatm. The strong oxygen super-saturation (AOU=−90 μmol kg^{-1}) and the low $NO_{3/2}$ and PO_4^{3-} concentrations in this area suggest that a phytoplankton bloom has developed there. This is confirmed by the higher chlorophyll concentrations of 4 to 5 μg L^{-1} present in this area compared to the remaining northern North Sea, where the average value was approximately 1 μg L^{-1}. The negative concentrations calculated for the excess DIC in this area also confirmed that strong biological production occurs in this area and reduces the DIC concentrations relative to the concentration expected with regard to the mixing line in Fig. 3.

At the stations near the Orkney (59.5°N; 2.5°W) and Shetland Islands (60°N; 1.7°W), the concentrations of DIC, nitrate and phosphate were higher than in the northern North Sea, with values of 2070 μmol kg^{-1} (Fig. 2E), 2.3 and 0.4 μmol L^{-1}, respectively. The water column at the station near the Orkney Islands was mixed down to the bottom (77 m) by strong tidal currents in this area (Turrell et al., 1992). Therefore, no export of POM is possible from the surface layer and this POM is remineralized in the deeply mixed surface layer, which promoted relatively high DIC concentrations at these stations.

4.3. The CO_2 system in the shallow southern North Sea

In the North Sea, south of 54°N, the surface distributions of pCO_2 and DIC (Fig. 2C and E) revealed higher concentrations than in the northern North Sea. The pCO_2 data have been normalized to a temperature of 16.5 °C representing the average surface water temperature during the cruise in order to eliminate the effects of different temperatures on the pCO_2 distribution (Fig. 2D). The distributions of the normalized and the in situ data showed a similar pattern, providing evidence that the higher surface water temperature in the southern North Sea was not primarily responsible for the higher pCO_2 in this area. These higher concentrations in the southern North Sea can be explained by the mixing regime of the water column. In this part of the North Sea, the water column is entirely mixed even in late summer because of the shallow depths and the strong tidal currents as high as 1 m s^{-1} (Eisma, 1987). During our late summer cruise, vertical profiles of salinity and temperature (not shown) did not show any stratification in this area (compare Fig. 4). The DIC profiles recorded at stations in the southern part of the North Sea, i.e., south of 54°N, showed a homogeneous concentration throughout the water column (Fig. 4A). Positive values of AOU (Figs. 4b and 5) associated with these higher concentrations of DIC suggest that remineralization of POM and/or inputs of brackish water, rich in organic matter occurred in the mixed water column, thus increasing the surface concentrations of DIC. This was confirmed by the moderate concentrations in $NO_{3/2}$ and PO_4^{3-} (Fig. 4C and D) observed throughout the water column for most stations in the Southern Bight and by the positive values calculated for excess DIC (Fig. 2F) in the surface layer of this area.

In the southern North Sea several stations, notably near the mouth of the Thames, Scheldt, Elbe and Humber estuaries, showed high DIC concentrations, where oxygen concentrations were slightly above the saturation level (Fig. 5). This suggests that the terrestrial water inputs, enriched in dissolved inorganic carbon and nutrients, stimulated primary pro-

duction within a narrow band of the coastal or estuarine waters. For example, the area situated in front of the Elbe estuary showed concentrations of DIC up to 2130 μmol kg^{-1} (Fig. 2E) and negative values for the excess DIC calculated for this area (Fig. 2F). This implies that the DIC concentrations found in this area are lower than expected with regard to the mixing line of brackish water from north European estuaries with Central North Sea water (Fig. 3). At these stations, the biological production dominates the remineralization of POM and induces an autotrophic state of the entirely mixed water column in a narrow band along the coast of the southern Bight.

To summarize, in most of the southern North Sea, the remineralization of POM dominates the biological production for the entire water column, which generates an overall heterotrophic state in late summer. Only at few stations along the coast influenced by riverine inputs from the main estuaries, the biological production dominates the remineralization of POM, which generates an autotrophic state of the water column.

4.4. The air–sea CO_2 fluxes during late summer

The flux (F) of CO_2 across the air–sea interface can be calculated using the formula:

$$F = k \times \alpha \times \Delta pCO_2 \quad (1)$$

where k is the gas transfer velocity, α is the solubility coefficient of CO_2 calculated after Weiss (1974) and ΔpCO_2 (pCO_{2water}–pCO_{2air}) is the air–water gradient of pCO_2. This parameterization implies that fluxes at the air–sea interface into the surface water (sink) are denoted with a negative sign, whereas fluxes into the atmosphere (source) are denoted by a positive sign. The gas transfer velocity is influenced by various factors such as air bubbles, surface films and air and water turbulence (Liss and Merlivat, 1986; Wanninkhof, 1992), but the wind speed has been recognised as the main force driving the gas exchange at the air–sea interface. Several algorithms have been proposed for the k–wind speed relationship. In our calculations, we use the k–wind speed relationships proposed by Liss and Merlivat (1986), Wanninkhof (1992), Wanninkhof and McGillis (1999), Nightingale et al. (2000a), Nightingale et al. (2000b), hereafter referred to as L&M86, W92 (short-term relationship), W&McG99 (short-term relationship), N2000a and N2000b, respectively. In fact, it is difficult to choose one relationship because even the latest experiments using the most recent tracer techniques applied for N2000a and N2000b could not reliably distinguish, which was the more favourable relationship. We therefore chose to report the results computed with the different formulations. This is particularly important for the North Sea in late summer, where two different features (e.g. super-saturation in the southern North Sea, under-saturation in the northern North Sea) have opposing effects on the overall fluxes of CO_2 for the whole area.

We computed the CO_2 fluxes employing the above different parameterizations of the gas transfer velocity, using two different data sets for wind speeds:

The in situ wind speeds recorded during the cruise were used to calculate instantaneous CO_2 fluxes. The wind speeds were corrected from 27 m (height of the vessel's anemometer) to 10 m using the relationship by Johnson (1999). The ΔpCO_2 values were calculated for the 22 000 surface water measurements, using an atmospheric partial pressure of CO_2 of 365 μatm, which was the average value of all the atmospheric measurements performed during the cruise. For each ΔpCO_2 observation, the CO_2 flux was calculated using the in situ wind speed and the different k parameterizations. The fluxes were interpolated onto a 0.05° by 0.05° grid in order to determine the flux for the two areas located between 51°N and 54°N and between 54°N and 60°N, as well as for the North Sea as a whole in late summer 2001 (Table 2).

We also used the six-hourly wind speed data from the European Centre for Medium-Range Weather Forecast (ECMWF) 40-years reanalysis project (ECMWF, 2002): The wind speed data were recalculated for our cruise by ECMWF from observations made in the North Sea for this period. The North Sea was divided in 13 boxes (Thomas et al., 2004). For each box, the gas transfer velocity was calculated every 6 h using ΔpCO_2 calculated from the measurements (Fig. 2C) and the wind speed from ECMWF. The fluxes were calculated for each of the 13 boxes, using the five different formulations. These results were then used to obtain the fluxes in the two above areas as well as for the North Sea as a whole (Table 2). In the following discussion, the first approach will refer to the calculations using the instantaneous wind

Table 2
The CO_2 fluxes calculated using the two different approaches: using the instantaneous winds speeds recorded on board (1) and the wind speed data recalculated for our cruise by ECMWF from observations made in the North Sea for this period (2)

	51°N–54°N	54 °N–60°N	North Sea
Range of pCO_2 (μatm)	287–487	190–448	190–487
Average ΔpCO_2 (μatm)	+26	−43	−26
Average of instantaneous wind speed (m s^{-1})	10.5	8.5	8.9
Monthly average wind speed ECMWF (m s^{-1})	7.8	8.2	8.1
Fluxes of CO_2 (mmol m^{-2} day^{-1}) calculated using the algorithms by:			
L&M86 (1)	+3.7	−3.9	−2.1
(2)	+0.8	−2.4	−1.5
W92 (1)	+6.3	−6.3	−3.4
(2)	+1.7	−3.2	−1.6
W&Mc99 (1)	+8.3	−5.0	−1.8
(2)	+0.8	−2.9	−1.8
N2000a (1)	+4.8	−5.2	−2.8
(2)	+1.4	−3.8	−2.2
N2000b (1)	+4.6	−4.7	−2.5
(2)	+1.3	−3.4	−2.0

Positive values denote fluxes into the atmosphere, whereas negative values denote fluxes into the surface water of the North Sea. L&M86 is the formulation from Liss and Merlivat (1986); W92 is the short-term formulation given by Wanninkhof (1992); W&Mc99 is the short-term formulation given by Wanninkhof and McGillis (1999); N2000a corresponds to the formulation given by Nightingale et al. (2000a); and N2000b is the formulation given by Nightingale et al. (2000b).

speeds, whereas the second approach will refer to the calculations using the six-hourly wind speed from the ECMWF project.

For the southern North Sea, the results obtained using the first approach are a factor of 5 to 6 higher than the results obtained with the second approach (Table 2). For this area, this large difference in the results is mainly due to the difference between the instantaneous wind speeds recorded on board and the actual wind speeds given by the ECMWF project for the time of observation. An event of strong winds (up to 25 m s^{-1}) occurred when sampling the southern area. Therefore, the average of instantaneous wind speeds recorded along the cruise track in this area was 10.5 m s^{-1}, not typical for this period of the year, when the six-hourly ECWMF wind speed was on average 7.8 m s^{-1} for the whole month and the entire southern area. The CO_2 air–sea flux calculation using the instantaneous wind speed on a monthly basis is thus biased by the above storm event, which is extrapolated to the entire area. Associated with high surface pCO_2, these high wind speeds are responsible for the much higher fluxes calculated in this area using the first approach. This implies that the extrapolation of instantaneous wind speed is not reliable for budgeting the CO_2 fluxes.

The fluxes obtained with the instantaneous wind speeds range from +3.7 to +8.3 mmol m^{-2} day^{-1} using L&M86 and W&Mc99, respectively (Table 2). This large difference is due to the different formulations of the L&M86 and W&Mc99 relationships between gas exchange and wind speed. The L&M86 can be closely approximated by a quadratic relationship over a wind speed range of 0–15 m s^{-1} whereas the W&Mc99 relationship is a cubic relationship between the wind speed and the gas transfer velocity. For both relationships, the gas transfer increases at an exponential rate as a function of the wind speed, which explains the large difference in the calculations. On the other hand, for the second approach, the value of +0.8 mmol m^{-2} day^{-1} found with W&Mc99 is in the same range of values obtained with the other formulations. The six-hourly reanalysis wind speeds tend to average out the very extreme events through spatial and temporal gridding processes. As a consequence, the wind speeds from ECMWF are in a range of value where the L&M86 and W&Mc99 calculations give similar values for the gas transfer velocity.

For the northern North Sea, results from the two different approaches are in rather good agreement. Fluxes calculated using the instantaneous wind speeds range from −3.9 to −6.3 mmol m^{-2} day^{-1} for L&M86 and W92, respectively, whereas in the second approach fluxes range from −2.4 to −3.8 mmol m^{-2} day^{-1} for L&M86 and N2000a, respectively. The slightly higher fluxes calculated using the first approach are surely due to the slightly higher average instantaneous wind speed (8.5 m s^{-1}) compared to the ECMWF average wind speed (8.2 m s^{-1}). The comparison of the two approaches shows that fluxes calculated from instantaneous wind speeds should only be used when the wind speeds recorded are typical of the meteorological conditions usually encountered in the studied area. For in situ investigations, the application of the instantaneous fluxes is obvious, whereas for budgeting approaches these

fluxes depend too much on the local and in situ weather situation. Therefore, for budgeting approaches it appears to be more reasonable to refer to CO_2 fluxes obtained using high-resolution wind field data for the time of observation. For the following discussion, we will thus only focus on the fluxes calculated with our second approach using the ECMWF wind speed data.

For the southern North Sea, the average ΔpCO_2 was +26 μatm, with a maximum value of +122 μatm (Fig. 2C). Therefore, the results from the five formulations show that the area situated between 51°N and 54°N releases CO_2 into the atmosphere at a rate between +0.8 and +1.7 mmol m^{-2} day^{-1} during late summer. On the other hand, the northern area showed an average ΔpCO_2 of −43 μatm, with areas strongly under-saturated like in the Skagerrak with ΔpCO_2 values of −176 μatm (Fig. 2C). The results from the five formulations show that the area situated between 54°N and 60°N absorbs CO_2 at a rate ranging from −2.4 to −3.8 mmol m^{-2} day^{-1}. The North Sea as a whole acts as a sink of CO_2 for the atmosphere in late summer in the range of −1.5 to −2.2 mmol m^{-2} day^{-1}, despite the fact that at this time of the year, the southern part of the North Sea is a source of CO_2 for the atmosphere. This flux is lower than the values of −3.9 and −16.4 mmol m^{-2} day^{-1} found in May–June by Kempe and Pegler (1991) and Frankignoulle and Borges (2001), respectively, both using the L&M86. In those two studies, the surface waters of the southern bight of the North Sea were under-saturated in CO_2 compared to the atmosphere. Thus, this area was a sink of atmospheric CO_2 and enhanced the CO_2 uptake for the whole North Sea, which explains the higher fluxes reported by these authors. However, they confirmed that in the areas where the water column was entirely mixed (the Dogger Bank, for Kempe and Pegler, 1991), the surface water released CO_2 to the atmosphere. In our study in late summer, as explained in Section 4.3, the water column in the Southern Bight was completely mixed and remineralization of POM was responsible for the higher source of CO_2 in the whole southern bight of the North Sea.

Thomas and Schneider (1999), using the W92 algorithms found that the surface waters of the Baltic Sea act as a strong sink of CO_2 of approximately −6.4 mmol m^{-2} day^{-1} in summer. Similarly, Tsunogai et al. (1997, 1999) and Wang et al. (2000) found values between −1.8 and −4.7 mmol m^{-2} day^{-1} for the East China Sea using L&M86 and W92, respectively. Compared to the latter coastal seas and the results for the North Sea by Kempe and Pegler (1991) and Frankignoulle and Borges (2001) in early summer, our study shows that the North Sea acts as a weak sink of CO_2 for the atmosphere during late summer (mid August–September).

4.5. The North Sea: a continental shelf pump

Once the CO_2 has been absorbed by the North Sea in summer, the fundamental issue concerning its eventual fate is related to the water circulation in the North Sea. The dominant feature in the North Sea is an anticlockwise circulation entering the North Sea west and east of the Shetland Channel. The current turns north-eastward in the central North Sea before finally leaving the North Sea along the Norwegian coast (Fig. 6) (Thomas et al., 2003b). As a consequence of the circulation pattern, the most prevailing feature of the semi-enclosed North Sea is the short residence time of this water, which is less than 1 year (Lenhart and Pohlmann, 1997).

In the subsurface layer, the above strong remineralization of exported organic material increases the DIC concentrations and prevents carbon accumulation in the bottom sediments, which amounts to less than 1% of the primary production (De Haas, 1997; De Haas et al., 2002). Therefore, the inorganic carbon, which has been transported from the atmosphere into the subsurface layer, ultimately can be exported to the Atlantic Ocean. The transfer of atmospheric CO_2 from the atmosphere to the North Sea is evident from increasing specific DIC concentrations (water column inventory of DIC divided by the water column depth) along the pathway of the Atlantic Ocean water through the North Sea. Within the inflowing western branch, the specific DIC concentration increases in southward direction (Fig. 6A), whereas within the outflowing eastern branch, the specific DIC concentration increases northward (Fig. 6B). Comparing the idealised entrance and exit of the Atlantic Ocean water at the Shetland Islands and the Norwegian coast, respectively, also here an increase of the specific DIC can be observed between inflowing and outflowing waters (from west to east, Fig. 6C).

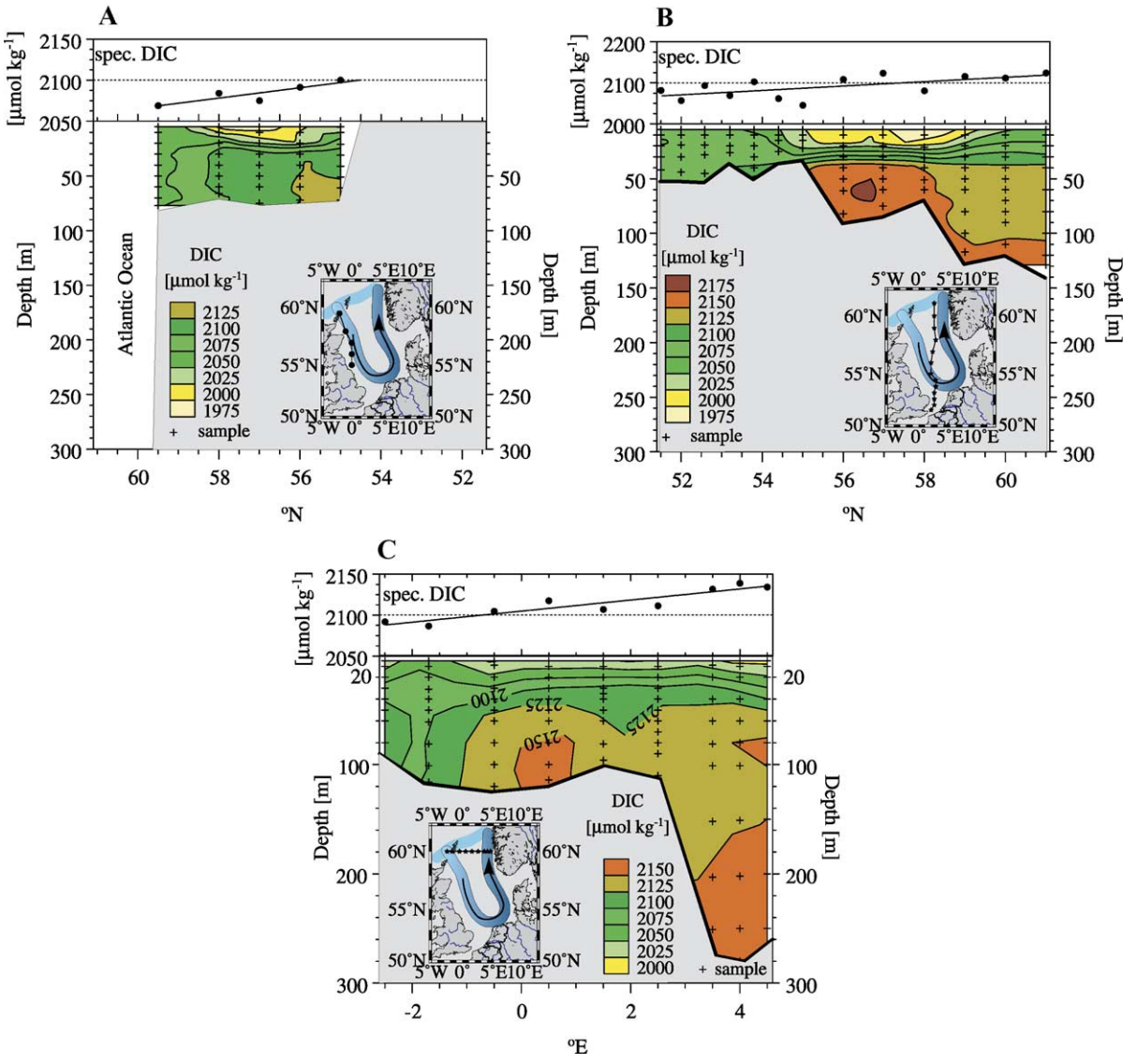

Fig. 6. Three sections of DIC (bottom panels) and specific DIC concentrations (top panels). Section on (A) covers the western, inflowing branch of the Atlantic Ocean circulation at approximately 0.5°W. The section on (B) covers the outflowing eastern branch at 2.5°E and the west–east section on (C) at 60°N shows the DIC concentrations at the entrance and at the exit, respectively. The underlying blue scheme indicates the general circulation and its darkening blue colour implies increasing DIC concentrations.

The specific DIC concentration in the Atlantic Ocean water mass increases by 40 µmol kg^{-1} during the transport through the North Sea (Fig. 6C). This DIC increase is generated both by the CO_2-uptake from the atmosphere and also by a net loss of dissolved organic carbon (DOC) in the northern North Sea as indicated by the higher DOC concentrations found in the inflowing compared to the outflowing waters (Thomas et al., 2004). Since the outflow of water along the Norwegian trench is 4725 km^3 $month^{-1}$ and this water is enriched with 40 µmol kg^{-1}, we estimate that 18.9×10^{10} mol C $month^{-1}$ is exported to the North Atlantic water during late summer when, at the same time, the North Sea

absorbs 2.8×10^{10} mol C month^{-1} from the atmosphere. Therefore, during late summer, the North Sea absorbs from the atmosphere a quantity of CO_2 equal to 15% of the carbon exported to the North Atlantic Ocean, implying that the North Sea acts as a continental shelf pump, further enhanced by heterotrophic activities.

With regard to the hypothesis of the continental shelf pump to the North Sea, the two major hydrographical regimes exert a major control, on whether and on how much CO_2 is transferred from the atmosphere to the adjacent North Atlantic Ocean (Fig. 7). For the shallower southern region, the biological carbon cycling occurs in the mixed surface layer. This means that biological production by algae and respiration processes by heterotrophic food web occur in the same compartment (Fig. 7) avoiding or diminishing net effects of the carbon cycling on the DIC concentrations in the water column, since no export of POM into the subsurface layer is possible. The obvious consequence for this is the observed super-saturation of the surface waters in the southern region (Fig. 2C). In contrast, in the northern region the stratification of the water column enables the export of POM from the surface layer to the deeper water column, thereby separating production from bacterial respiration processes. The POM is respired in the deeper layer and DIC is released. A net transport of carbon from the surface layer to the deeper layers occurs, which is ultimately replenished from the atmosphere. This is evident from the observed under-saturation of the surface waters in the northern region (Fig. 2C) as well as from the increasing DIC concentrations in the subsurface layer (Figs. 4A and 6). The subsurface layer is then subjected to water mass transport to the North Atlantic Ocean (Fig. 7), finally a net CO_2 transport from the atmosphere to the North Atlantic Ocean takes place.

5. Summary

The distributions of DIC and pCO_2 in the North Sea in late summer are mainly driven by the mixing regime of the water column influenced by the bottom topography of the North Sea. A clear boundary is evident in the distribution of DIC and pCO_2 as well as for related parameters such as AOU, $NO_{3/2}$ and PO_4 at 54°N. South of this border, the strong tidal currents mix the entirely shallow water column down to the bottom. By consequence, the degradation of POM releases inorganic carbon into the surface water of this area. North of 54°N, the deeper water column is stratified, which results in a spatial separation of biological carbon uptake in the surface layer and degradation of POM in the bottom layer.

In the Southern Bight, inputs of less saline water from the major European estuaries with high inorganic carbon content increase the surface water concentration of DIC along the coast. In the northern part, inputs of less saline water from the Baltic Sea

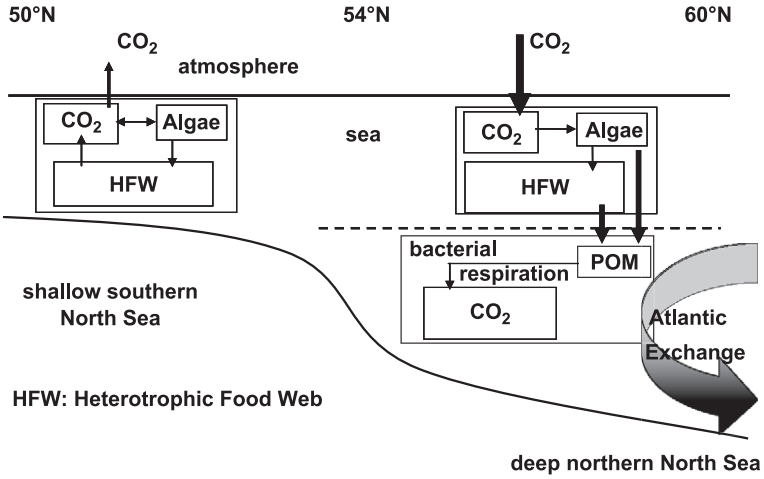

Fig. 7. Schematic representation of the mechanism of the continental shelf pump in the North Sea. Redrawn after Thomas et al. (2004).

with a low DIC content dilute the dissolved inorganic carbon concentrations.

The southern North Sea acts as a source of CO_2 for the atmosphere in late summer with fluxes of +0.8 to +1.7 mmol m^{-2} day^{-1}, whereas the northern part acts as a sink of CO_2 for the atmosphere at a rate of −2.4 to −3.8 mmol m^{-2} day^{-1}. The North Sea as a whole constitutes a sink of atmospheric CO_2 ranging from −1.5 to −2.2 mmol m^{-2} day^{-1} or 0.4×10^{12} g C $month^{-1}$ despite the source in the southern part. This atmospheric CO_2 increases the DIC content of the deeper layer of the water column via the biological pump. In late summer, the North Sea exports 2.2×10^{12} g C $month^{-1}$ to the North Atlantic Ocean via the Norwegian trench. During the same period, the North Sea takes up from the atmosphere a quantity of CO_2 equal to 15% of what is exported. The increase in DIC concentrations in the bottom layer is the result of CO_2 pumping occurring during the year and the remainder is generated by heterotrophic activities. During late summer, the North Sea thus acts as a continental shelf pump exporting the CO_2 taken up from the atmosphere to the North Atlantic Ocean.

Acknowledgements

The excellent co-operation of the captains and the crews of *RV Pelagia* as well as the scientific crew is gratefully acknowledged. We thank DKRZ, DWD and Dr. Johannes Pätsch for making available the ECMWF wind data. We are grateful to Prof. Leif Anderson and Dr. Rik Wanninkhof for their helpful comments on a previous version of our manuscript. This study has been encouraged by and contributes to the LOICZ core project of the IGBP. It has been supported by the Netherlands Organisation for Scientific Research (NWO), grants no. 810.33.004 and 014.27.001, and the Dutch–German bilateral co-operation NEBROC.

References

Bakker, D.C.E., de Baar, H.J.W., de Wilde, H.P.J., 1996. Dissolved carbon dioxide in Dutch coastal waters. Marine Chemistry 55 (3–4), 247–263.

Borges, A.V., Frankignoulle, M., 1999. Daily and seasonal variations of the partial pressure of CO_2 in surface seawater along Belgian and southern Dutch coastal areas. Journal of Marine Systems 19, 251–266.

Borges, A.V., Frankignoulle, M., 2002. Distribution and air–water exchange of carbon dioxide in the Scheldt plume off the Belgian coast. Biogeochemistry 59, 41–67.

Brasse, S., Reimer, A., Seifert, R., Michaelis, W., 1999. The influence of intertidal mudflats on the dissolved inorganic carbon and total alkalinity distribution in the German Bight, southeastern North Sea. Journal of Sea Research 42, 93–103.

Brasse, S., Nellen, M., Seifert, R., Michaelis, W., 2002. The carbon dioxide system in the Elbe estuary. Biogeochemistry 59, 25–40.

De Haas, H., 1997. Transport, preservation and accumulation of organic carbon in the North Sea. PhD thesis, Universiteit Utrecht, Utrecht, 149 pp.

De Haas, H., Van Weering, T.C.E., De Stigter, H., 2002. Organic carbon in shelf seas: sinks or sources, processes and products. Continental Shelf Research 22, 691–717.

ECMWF, 2002. 40-Year reanalysis of wind data ERA40. WWW Page, http://www.ecmwf.int.

Eisma, D., 1987. The North Sea: an overview. Philosophical Transactions of the Royal Society of London. B 316, 461–485.

Frankignoulle, M., Borges, A.V., 2001. European continental shelf as a significant sink for atmospheric carbon dioxide. Global Biogeochemical Cycles 15 (3), 569–576.

Frankignoulle, M., Bourge, I., Canon, C., Dauby, P., 1996a. Distribution of surface seawater partial CO_2 pressure in the English Channel and in the Southern Bight of the North Sea. Continental Shelf Research 16 (3), 381–395.

Frankignoulle, M., Bourge, I., Wollast, R., 1996b. Atmospheric CO_2 fluxes in a highly polluted estuary (the Scheldt). Limnology and Oceanography 41 (2), 365–369.

Frankignoulle, M., Elskens, M., Biondo, R., Bourge, I., Canon, C., Desgain, S., Dauby, P., 1996c. Distribution of inorganic carbon and related parameters in surface seawater of the English Channel during spring 1994. Journal of Marine Systems 7, 427–434.

Frankignoulle, M., Abril, G., Borges, A., Bourge, I., Canon, C., Delille, B., Libert, E., Théate, J.-M., 1998. Carbon dioxide emission from European estuaries. Science 282, 434–436.

Gattuso, J.-P., Frankignoulle, M., Wollast, R., 1998. Carbon and carbonate metabolism in coastal aquatic ecosystems. Annual Reviews of Ecological Systems 29, 405–434.

Grasshoff, K., Ehrhardt, M., Kremling, K., 1983. Methods of Seawater Analysis (2nd ed.). Verlag Chemie, Weinheim.

Gruber, N., Keeling, C.D., 2001. An improved estimate of the isotopic air–sea disequilibrium of CO_2: implications for the oceanic uptake of anthropogenic CO_2. Geophysical Research Letters 28 (3), 555–558.

Holm-Hansen, O., Lorenzen, C.J., Homes, R.W., Strickland, J.D.H., 1965. Fluorometric determination of chlorophyll. Journal de Conseil pour l'Exploration de la Mer 30 (1), 3–15.

Hoppema, J.M.J., 1990. The distribution and seasonal variation of alkalinity in the Southern Bight of the North Sea and in the western Wadden Sea. Netherlands Journal of Sea Research 26 (1), 11–23.

Hoppema, J.M.J., 1991. The seasonal behaviour of carbon dioxide and oxygen in the coastal North Sea along the Netherlands. Netherlands Journal of Sea Research 28 (3), 167–179.

IPCC, 2001. The scientific basis. In: Houghton, J.T., et al. (Eds.), Contribution of Working Group I to the Third Assessment Report of the Intergovernmental Panel on Climate Change. Cambridge University Press, New York, USA.

Johnson, H.K., 1999. Simple expressions for correcting wind speed data for elevation. Coastal Engineering 36, 263–269.

Johnson, K.M., Wills, K.D., Butler, D.B., Johnson, W.K., Wong, C.S., 1993. Coulometric total carbon dioxide analysis for marine studies: maximizing the performance of an automated gas extraction system and coulometric detector. Marine Chemistry 44, 167–187.

Kempe, S., 1995. Coastal seas: a net source or sink of atmospheric carbon dioxide? LOICZ/R and S/95-1, vi+27 pp. LOICZ, Texel, The Netherlands.

Kempe, S., Pegler, K., 1991. Sinks and sources of CO_2 in coastal seas: the North Sea. Tellus 43B, 224–235.

Kempe, S., Liebezeit, V., Dethlefsen, V., Harms, U., 1988. Biogeochemistry and distribution of suspended matter in the North Sea and implications to Fisheries Biology. Inst. Univ. Hamburg, Heft, vol. 65. 552 pp.

Körtzinger, A., Thomas, H., Schneider, B., Gronau, N., Mintrop, L., Duinker, J.C., 1996. At-sea intercomparison of two newly designed underway pCO_2 systems—encouraging results. Marine Chemistry 52, 133–145.

Lee, K., Wanninkhof, R.H., Takahashi, T., Doney, S., Feely, R.A., 1998. Low interannual variability in recent oceanic uptake of atmospheric carbon dioxide. Nature 396, 155–159.

Lenhart, H., Pohlmann, T., 1997. The ICES-boxes approach in relation to results of a North Sea circulation model. Tellus 49A (1), 139–160.

Liss, P.S., Merlivat, L., 1986. Air–sea gas exchange rates: Introduction and synthesis. In: Buat-Ménard, P. (Ed.), The Role of Air–Sea Exchange in Geochemical Cycling. D. Reidel Publishing, pp. 113–127.

Mackenzie, F.T., Lerman, A., Ver, L.M., 1998. Role of continental margin in the global carbon balance during the past three centuries. Geology 26 (5), 423–426.

Nightingale, P.D., Liss, P.S., Schlosser, P., 2000a. Measurements of air–sea gas transfer during an open ocean algal bloom. Geophysical Research Letters 27 (14), 2117–2120.

Nightingale, P.D., Malin, G., Law, C.S., Watson, A.J., Liss, P.S., Liddicoat, M.I., Boutin, J., Upstill-Goddard, R.C., 2000b. In situ evaluation of air–sea gas exchange parameterizations using novel conservative and volatile tracers. Global Biogeochemical Cycles 14 (1), 373–387.

Orr, J.C., Maier-Reimer, E., Mikolajewicz, U., Monfray, P., Sarmiento, J.L., Toggweiler, J.R., Taylor, N.K., Palmer, J., Gruber, N., Sabine, C.L., Le Quéré, C., Key, R.M., Boutin, J., 2001. Estimates of anthropogenic carbon uptake from four three-dimensional global ocean models. Global Biogeochemical Cycles 15 (1), 43–60.

Osterroht, C., Thomas, H., 2000. New production enhanced by nutrient supply from non-Redfield remineralisation of freshly produced organic material. Journal of Marine Systems 25, 33–46.

Pegler, K., Kempe, S., 1988. The carbonate system of the North Sea: determination of alkalinity and TCO_2 and calculation of PCO_2 and Sl_{cal} (spring 1986). Mitteilungen aus dem Geologisch-Paläontologischen Institut der Universität Hamburg 65, 35–87.

Postma, H., Rommets, J.W., 1984. Variations of particulate organic carbon in the Central North Sea. Netherlands Journal of Sea Research 18 (31 pp.).

Smith, S.V., Hollibaugh, J.T., 1993. Coastal metabolism and the ocean organic carbon balance. Reviews of Geophysics 31 (1), 75–89.

Stoll, M.H.C., 1994. Inorganic carbon behaviour in the North Atlantic Ocean. PhD thesis, Rijksuniversiteit Groningen, Groningen, 193 pp.

Thomas, H., Schneider, B., 1999. The seasonal cycle of carbon dioxide in the Baltic Sea surface waters. Journal of Marine Systems 22, 53–67.

Thomas, H., Ittekkot, V., Osterroht, C., Schneider, B., 1999. Preferential recycling of nutrients—the ocean's way to increase new production and to pass nutrient limitation? Limnology and Oceanography 44 (8), 1999–2004.

Thomas, H., England, M.H., Ittekkot, V., 2001. An off-line 3D model of anthropogenic CO_2 uptake by the oceans. Geophysical Research Letters 28 (3), 547–550.

Thomas, H., Pempkowiak, J., Wulff, F., Nagel, K., 2003a. Autotrophy, nitrogen accumulation and nitrogen limitation in the Baltic Sea: a paradox or a buffer for eutrophication? Geophysical Research Letters 30 (21), 2130–2133.

Thomas, H., Gattuso, J.-P., Smith, S.V., 2003b. Coastal Biogeochemistry at the EGS–AGU–EUG Joint Assembly, Nice, France, 6–11 April 2003, LOICZ Newsletter, vol. 28. LOICZ, Texel, The Netherlands.

Thomas, H., Bozec, Y., Elkalay, K., De Baar, H., 2004. Enhanced open ocean storage of CO_2 from shelf sea pumping. Science 304, 1005–1008.

Tsunogai, S., Watanabe, S., Nakamura, J., Ono, T., Sato, T., 1997. A preliminary study of carbon system in the East China Sea. Journal of Oceanography 53, 9–17.

Tsunogai, S., Watanabe, S., Sato, T., 1999. Is there a "continental shelf pump" for the absorption of atmospheric CO_2? Tellus 51B, 701–712.

Turrell, W.R., Henderson, E.W., Slesser, G., Payne, R., Adams, R.D., 1992. Seasonal changes in the circulation of the northern North Sea. Continental Shelf Research 12 (2/3), 257–286.

Walsh, J.J., 1991. Importance of continental margins in the marine biogeochemical cycling of carbon and nitrogen. Nature 350, 53–55.

Wang, S.-L., Chen, C.-T.A., Hong, G.-H., Chung, C.-S., 2000. Carbon dioxide and related parameters in the East China Sea. Continental Shelf Research 20, 525–544.

Wanninkhof, R., 1992. Relationship between wind speed and gas exchange over the ocean. Journal of Geophysical Research 97 (C5), 7373–7382.

Wanninkhof, R., McGillis, W.R., 1999. A cubic relationship between air–sea CO_2 exchange and wind speed. Geophysical Research Letters 26 (13), 1889–1892.

Weiss, R.F., 1970. The solubility of nitrogen, oxygen and argon in water and seawater. Deep-Sea Research 17, 721–735.

Weiss, R.F., 1974. Carbon dioxide in water and seawater: the solubility of a non-ideal gas. Marine Chemistry 2, 203–215.

Wollast, R., 1998. Evaluation and comparison of the global carbon cycle in the coastal zone and in the open ocean. In: Brink, K.H., Robinson, A.R. (Eds.), The Sea. John Wiley & Sons, New York, pp. 213–252.